Electronic Supplementary Material

Versatile multiplexed super-resolution imaging of nanostructures by Quencher-Exchange-PAINT

Tobias Lutz[1], Alexander H. Clowsley[1], Ruisheng Lin[1], Stefano Pagliara[1], Lorenzo Di Michele[2], and Christian Soeller[1] (✉)

[1] *Living Systems Institute & Biomedical Physics, University of Exeter, Exeter EX4 4QD, UK*
[2] *Cavendish Laboratory, University of Cambridge, Cambridge CB3 0HE, UK*

Supporting information to https://doi.org/10.1007/s12274-018-1971-6

SUPPLEMENTARY THEORY. Background fluorescence in a chemical equilibrium of bound and unbound complementary imager and quencher strand pairs in solution can be described by

$$F \propto [I] + \alpha [IQ] + \beta [Q] + \gamma \qquad \text{Eq. (S1)}$$

with $[I]$ being the concentration of free, i.e. single stranded imager, $[Q]$ the concentration of single stranded quencher strands, $[IQ]$ the concentration of the hybridised imager-quencher complex and the factors α describing the ratio of single molecule fluorescence of an imager-quencher complex to a free imager, while β is the ratio of single molecule fluorescence of a free quencher to a free imager. γ is a parameter that accounts for any additional constant background fluorescence, e.g. from free dye molecules or dye attached to non-complementary oligos.

With $[I_0]$ the total concentration of imager strands, free or in IQ complex and $[Q_0]$ the total concentration of quencher strands, free or in IQ complex, the concentration of the imager-quencher complex $[IQ]$ can be calculated as a function of $[I_0]$, $[Q_0]$ and the dissociation constant K_d,

$$K_d = \frac{[I][Q]}{[IQ]}$$

$$K_d = \frac{([I_0]-[IQ])([Q_0]-[IQ])}{[IQ]}$$

$$[IQ]_{1,2} = \frac{[I_0]+[Q_0]+K_d}{2} \pm \sqrt{\frac{([I_0]+[Q_0]+K_d)^2}{2} - [I_0][Q_0]} \qquad \text{Eq. (S2)}$$

Address correspondence to c.soeller@exeter.ac.uk

with only $[IQ]=\ldots-\sqrt{\ldots}$ giving non-negative concentrations.

This results in a fluorescence intensity of

$$\begin{aligned} F &\propto [I]+\alpha[IQ]+\beta[Q]+\gamma \\ &=[I_0]+(\alpha-\beta-1)[IQ]+\beta[Q_0]+\gamma \\ &=[I_0]+(\alpha-\beta-1)\left(\frac{[I_0]+[Q_0]+K_d}{2}-\sqrt{\frac{([I_0]+[Q_0]+K_d)^2}{2}-[I_0][Q_0]}\right)+\beta[Q_0]+\gamma, \end{aligned} \quad \text{Eq. (S3)}$$

The binding-event rate upon addition of a complementary quencher strand is proportional to the concentration of free imager $[I_0]$ which in equilibrium depends on $[I_0]$ and $[Q_0]$ as shown above.

For quencher-imager binding with high affinity $K_d = [I_0],[Q_0]$, the free imager concentration can be approximated by

$$\begin{aligned} [I]=[I_0]-[IQ]&=\frac{[I_0]-[Q_0]-K_d}{2}+\sqrt{\frac{([I_0]+[Q_0]+K_d)^2}{4}-[I_0][Q_0]} \\ &\approx [I_0]-[Q_0], (K_d = [I_0],[Q_0]) \end{aligned} \quad \text{Eq. (S4)}$$

supplementary figures.

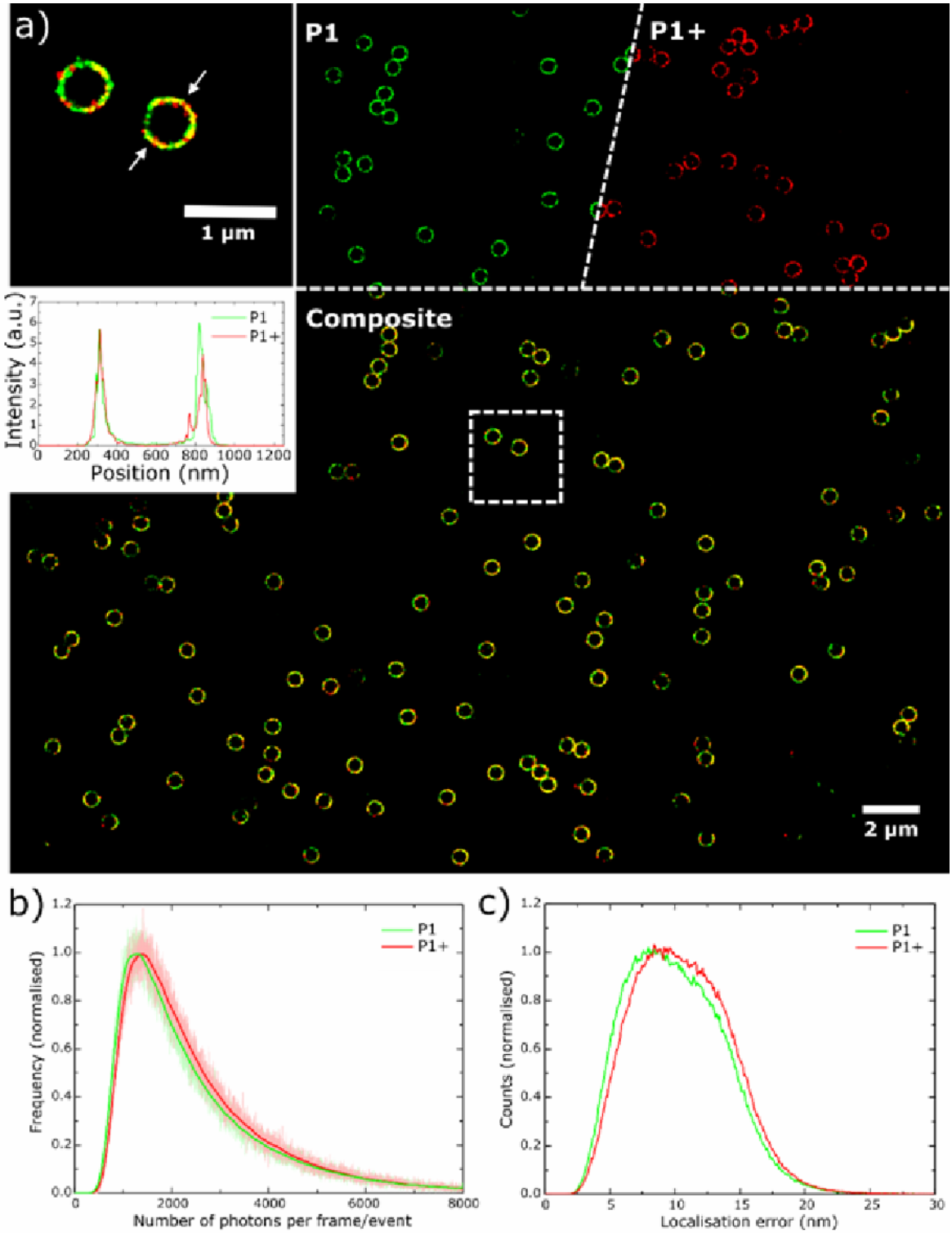

Figure S1 Comparison of extended Imager P1+ with P1 by Exchange-PAINT imaging of Ø = 500 nm polystyrene beads. a) Composite Exchange-PAINT image using imager P1 (green) and P1+ (red). Top left: Magnified view of the boxed region. Inset: Cross section of an individual bead indicated by the arrows. b) Histogram showing the number of detected photons per frame and binding event. c) Histogram of the localisation error for imagers P1 and P1+.

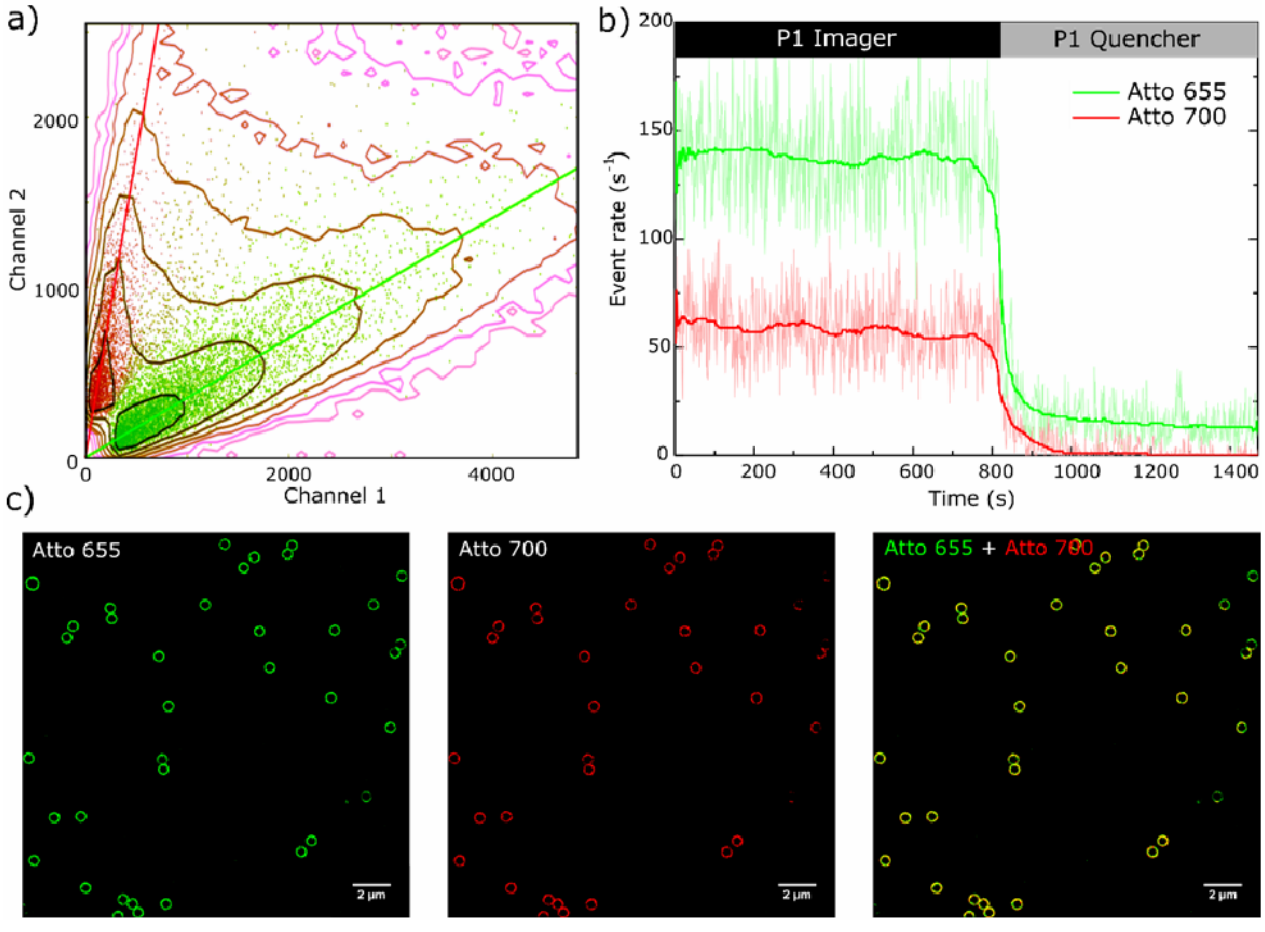

Figure S2 Spectrally multiplexed DNA-PAINT in combination with quencher strands as a proof-of-principle experiment demonstrating the possibility of a combination of multi-colour imaging with Quencher-Exchange-PAINT. Streptavidin-coated polystyrene beads labelled with P1 docking strands were imaged simultaneously by two types of P1 imagers modified with Atto 655 and Atto 700, respectively. The two colour channels were separated with a dichroic mirror (DC/T710 LPXXR-UF3, Chroma) and imaged on either half of an EMCCD camera chip (Andor iXon Ultra DV97). a) The intensity plot of both channels shows that the emission of Atto 655 (green) and Atto 700 (red) can be clearly separated. b) The complementary quencher strand hybridises to the P1 imagers independently of the dye modification and thus reduces the detection event rate in both channels. In principal, different imager/quencher sequence pairs could be used and additional, orthogonal imager strands could be added after a quenching step to increase the number of detected targets. c) Rendered images of the Atto 655 channel (green), the Atto 700 channel (red) and an overlay, which demonstrates a strong correlation between the two channels.